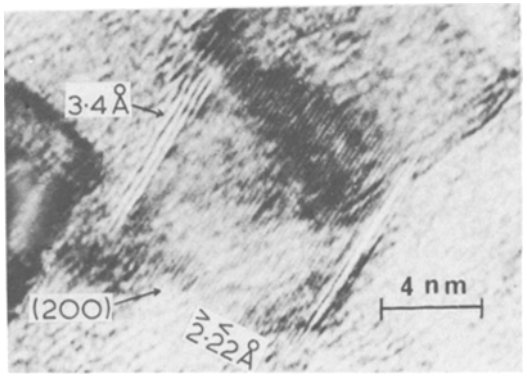

Figure 4 Graphite deposits on (2 0 0) TaC planes.

conditions, on the other hand, Ta_2C can be completely eliminated as mentioned, and the tantalum monocarbide crystals have a tendency to be smaller and more easily identifiable. Fig. 3 shows a typical high resolution electron micrograph of a material prepared under such conditions. The stoichiometric TaC grains are embedded in an amorphous carbon matrix, which probably acts as a protection against oxidation and is thought to be responsible for the rather low oxygen contents recorded here (Table II). On closer examination (Fig. 4), many crystals appear as fairly well formed cubes, the faces of which correspond to the {1 0 0} crystal planes, as indicated by the measured interplanar spacing (Fig. 4). Also, on some of these cube planes, graphite-like deposits a few layers thick, (interplanar spacing: 3.4 Å) are visible.

In summary, the present work is believed to show that ultrafine TaC powders can be prepared under conditions allowing higher purities to be achieved than seems to be commonly possible when arc-plasma or chemical vapour-deposition techniques are used. The presence of sizable amounts of excess carbon appears to be helpful as a protection against oxidation and possibly as a dispersing medium for the carbide particles.

Acknowledgements

This work was supported by Société: Le Carbone-Lorraine. The high resolution electron micrographs (Figs. 3 and 4) were obtained by Mme Oberlin (C.N.R.S. – Orléans), and kindly provided by Drs J. P. Slonina and J. Maire of Carbone-Lorraine.

References

1. C. S. STOKES, J. A. CAHILL, J. J. CORREA and A. V. GROSSE, Final Report, Grant 62-196, A.F. Office of Scientific Research (1965).
2. E. NEUENSCHWANDTER, *J. Less Common Metal* **11** (1966) 365.
3. J. SAUTEREAU and A. MOCELLIN, *J. Mater. Sci.* 9 (1974) 761.
4. J. CANTELOUP and A. MOCELLIN, "Special Ceramics 6" edited by P. Popper (B.C.R.A., Stoke-on-Trent, 1975) p. 209.

Received 6 July
and accepted 27 July 1976

J. CANTELOUP
A. MOCELLIN
Centre des Matériaux,
Ecole des Mines de Paris,
B.P. 87–91003 Evry-Cedex,
France

Slow surface crack growth during Vickers indentation on glass

The indentation fracture of glass and other brittle materials has been the topic of several recent publications [1–3]. Although cracks have been observed to form beneath the surface of glass during Vickers indentation, the growth of surface cracks during the loading half of the indentation cycle has been a matter of speculation. Almond [4] has observed cracks growing from the corners of Vickers indents in carbides by performing the indentation experiments in a scanning electron microscope, but this technique is not suitable for non-conductors.

A set of indentation experiments performed in these laboratories under unusual conditions has thrown some light on the problem. A bench model Instron testing machine with a Vickers diamond mounted from the cross-head was used to indent a glass block. There was no damping material underneath the Instron, and so the vibration of the motor was transmitted through the frame of the testing machine to the cross-head. Subsequent measurements of the deflection of the cross-head using a displacement transducer indicated that there was a load fluctuation of $\pm\frac{1}{2}\%$ at an applied load of 5 kg.

The Vickers indent formed at 5 kg on glass by this method was very poor (Fig. 1), but it pos-

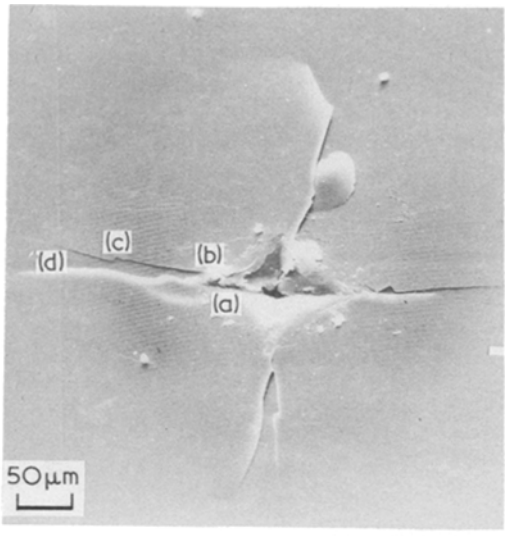

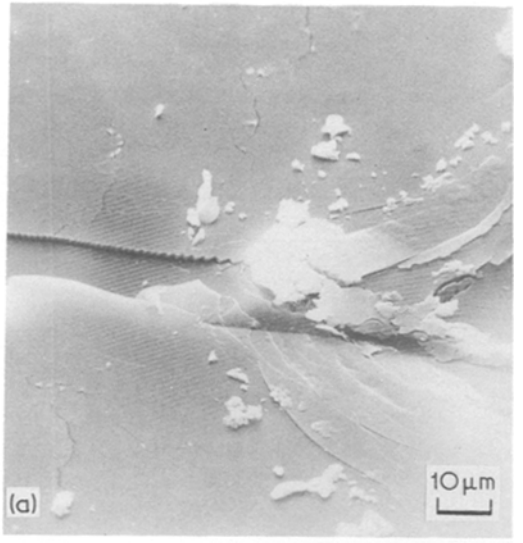

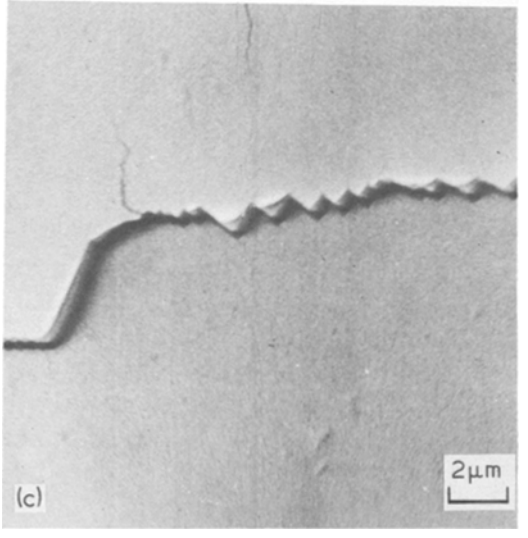

sessed several interesting features. Fig. 1a shows a serrated crack leaving the centre of the residual impression and running close to, but not along, the diagonal of the indent. This crack must have been initiated at a load considerably less than the peak load of 5 kg and its divergence from the diagonal indicates that the Vickers pyramid is probably not perpendicular to the surface of the glass. The serrations in the crack (Fig. 1b) are caused by the fluctuating load from the cross-head of the Instron and demonstrate that the crack is propagating slowly as the load increases. This is analogous to the ultrasonic technique for measuring rapid crack

Figure 1 Regions of slow and fast crack growth from the corners of a Vickers indent on glass: (a) crack initiation, (b) slow propagation, (c) transition, and (d) rapid propagation.

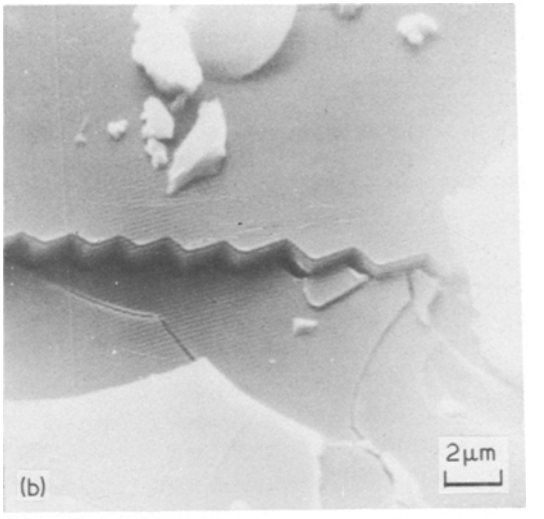

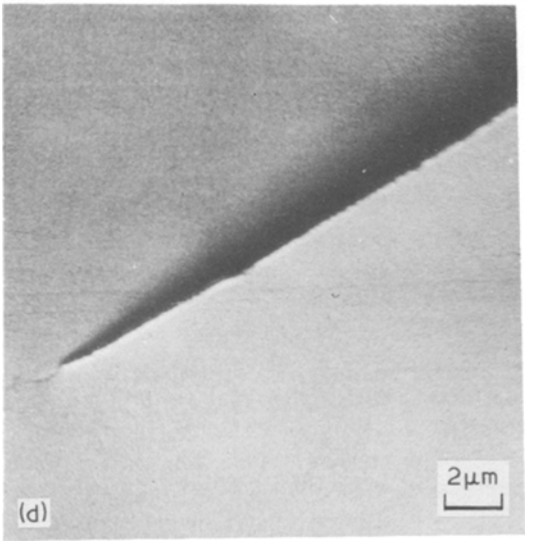

velocities in brittle materials [5]. Approximately half-way along the final crack there is a transition (Fig. 1c) from a serrated to a smooth crack (Fig. 1d), and this transition point is the limit of slow crack growth on loading. The velocity of the crack, calculated from the size of the serrations, is 6×10^{-3} m min^{-1} when the cross-head speed on the Instron is 5×10^{-5} m min^{-1}.

This slow surface crack growth occurs simultaneously with the formation of median vents [6]. The median vent is an internal penny-shaped crack lying in the same plane as the surface crack but separate from it. On unloading or at high applied loads the penny-shaped median vent runs to the surface joining the surface corner crack and forming a semi-circular crack. The smooth crack extending beyond the transition point (Fig. 1c and d) is due to the median vent breaking through to the surface. Similar experiments with cone indenters showed no sign of slow crack growth, which suggests that surface cracks associated with such indents are only formed by median vents running to the surface at high loads or on unloading, and that the slow crack growth reported here is due to stress concentration around the corners of the Vickers indenter.

References

1. B. R. LAWN and T. R. WILSHAW, *J. Mater. Sci.* **10** (1975) 1049.
2. B. R. LAWN, M. V. SWAIN and K. PHILLIPS, *ibid* **10** (1975) 1236.
3. B. R. LAWN and E. R. FULLER, *ibid* **10** (1975) 2016.
4. E. A. ALMOND and B. ROEBUCK, "Scanning Electron Microscopy: systems and applications" (Institute of Physics, London, 1973) pp. 106–11.
5. J. E. FIELD, *Contemp. Phys.*, **12** (1) (1971) 1.
6. K. PHILLIPS, D. Phil. Thesis, University of Sussex (1975).

Received 12 July
and accepted 27 July 1976

K. PHILLIPS*
School of Engineering and Applied Sciences,
University of Sussex,
Brighton, Sussex, UK

* Present address: Department of Metallurgy and Materials Technology, University of Surrey, Guildford, Surrey, UK.

Molecular mechanisms in annealing of oriented polypropylene

Deformation mechanisms in oriented crystalline polymers have been studied using a combination of low-angle X-rays (LAXP) and wide-angle X-rays (WAXP) [1–3]. In the present note, similar techniques have been applied to the study of mechanisms by which these materials change lamellar orientation on annealing after deformation.

The various deformation mechanisms in oriented crystalline polymers have been examined in some detail [1–3]. The mechanisms are those involving shear processes (intermolecular, interlamellar and interfibrillar), normal processes (interlamellar separation or fibrillar separation) and twinning processes within the lamellae. In oriented polypropylene, both X-ray diffraction and yield behaviour studies have shown the predominance of the intermolecular shear process in room temperature deformation [3]. This has been demonstrated for a range of orientations of approximately $20° < \theta_0 < 70°$ (where θ_0 is the angle between the molecular axis and the tensile axis).

Commercially obtained polypropylene sheet was hot drawn in air at 150° C to a total residual strain of ~ 600%. Tensile specimens of the standard "dumb-bell" shape were cut from this material at an angle $\theta_0 = 31°$ which was within the range of intermolecular shear on tensile deformation. These were ground and polished to approximately 0.5 mm thickness. The specimens were mounted in a small tensile jig suitable for *in situ* low- and wide-angle X-ray studies [3]. The jig was constructed so that it could be removed, with the specimen under load, and the specimen annealed in an oil bath. Thus the specimen was constrained by fixed grips.

A specimen was deformed in tension to a strain of 64% and annealed in a series of steps as follows:

Time at temperature (h)	Annealing temperature (° C)
1	100
1	100
1	130
1	140